Development 128, 2603-2614 (2001)
Printed in Great Britain © The Company of Biologists Limited 2001
DEV4544

Extranuclear sequestration of phospho-Jun N-terminal kinase and distorted villi produced by activated Rac1 in the intestinal epithelium of chimeric mice

Thaddeus S. Stappenbeck[1,2] and Jeffrey I. Gordon[1]

[1]Department of Molecular Biology and Pharmacology, Washington University School of Medicine, St. Louis, MO 63110, USA
[2]Department of Pathology and Immunology, Washington University School of Medicine, St. Louis, MO 63110, USA
*Author for correspondence (e-mail: jgordon@molecool.wustl.edu)

Accepted 17 April 2001

SUMMARY

Previously, we used a genetic mosaic system to conduct an in vivo analysis of the effects of Rac1 activation on the developing intestinal epithelium (Stappenbeck, T. S. and Gordon, J. I. (2000) *Development* 127, 2629-2642). Expression of a constitutively active human Rac1 (Rac1Leu61) in the 129/Sv-derived small intestinal epithelium of C57Bl/6-ROSA26↔129/Sv chimeric mice led to precocious differentiation of some lineages with accompanying alterations in their apical actin. We have now explored the underlying mechanisms. Rac1Leu61 leads to accumulation of the 46 kDa form of phosphorylated Jun N-terminal kinase (p-Jnk) in the apical cytoplasm, but not in the nucleus of E18.5 proliferating and differentiating intestinal epithelial cells. The effect is cell-autonomous, selective for this mitogen-activated protein kinase family member, and accompanied by apical cytoplasmic accumulation of p21-activated kinase. c-Jun, a downstream nuclear target of p-Jnk, does not show evidence of enhanced phosphorylation, providing functional evidence for cytoplasmic sequestration of p-Jnk in Rac1Leu61-expressing epithelium. In adult chimeras, Rac1 activation augments cell proliferation in crypts of Lieberkühn, without a compensatory change in basal apoptosis and produces a dramatic, very unusual widening of villi. These results reveal a novel in vivo paradigm for Rac1 activation involving p-Jnk-mediated signaling at a distinctive extra-nuclear site, with associated alterations in the actin cytoskeleton. They also provide a new perspective about the determinants of small intestinal villus morphogenesis.

Key words: Rac, MAP kinases, Actin, Mouse, Intestine, Epithelium

INTRODUCTION

The mouse small intestinal epithelium is an appealing system for studying the influence of specific signal transduction pathways on proliferation, differentiation and migration. In the adult, proliferation is confined to well-defined anatomic units known as crypts of Leiberkühn. Several active, long-lived multipotential stem cells are anchored at or near the base of each crypt (Wong et al., 2000). These stem cells produce committed daughters that form a transit amplifying population of rapidly dividing cells located in the middle of the crypt (Wong et al., 2000; Bjerknes and Cheng, 1999; Booth and Potten, 2000). Differentiation occurs rapidly and is associated with an orderly migration of the four epithelial cell lineages of the small intestine. Members of one lineage (Paneth cell) complete their differentiation as they move to the crypt base (Cheng, 1974b). Members of the other three lineages (enterocytic, goblet and enteroendocrine) differentiate as they move out of crypts, onto and up adjacent finger-like villi (Cheng, 1974a; Cheng and Leblond, 1974a; Cheng and Leblond, 1974b; Cheng and Leblond, 1974c; Schmidt et al., 1985). Enterocytes represent the dominant lineage. A key feature of their differentiation is assembly of an actin cytoskeleton and associated proteins in the apical cytoplasm to form a mature brush border. As enterocytes, goblet and enteroendocrine cells approach the apex of a villus, they are lost by apoptosis and/or exfoliation (Hall et al., 1994).

The crypt-villus units that support this epithelial renewal are fully formed by the second postnatal week. In late fetal life, rudimentary villi appear, cell division is confined to the intervillus region, and differentiated members of the enterocytic, goblet and enteroendocrine lineages arise. Crypt morphogenesis takes place during the first two postnatal weeks (Calvert and Pothier, 1990; Schmidt et al., 1988), at which time mature Paneth cells become evident (Bry et al., 1994). Proper development of crypt-villus units reflects a complex crosstalk between the epithelium and the underlying mesenchyme**.** For example, it appears that platelet-derived growth factor A (PDGF-A) secreted from the fetal epithelium stimulates proliferation and clustering of PDGF receptor-α-expressing mesenchymal cells that serve as signaling centers to promote formation of villi (Karlsson et al., 2000). Indian hedgehog also functions as an important mediator of the endodermal mesenchymal crosstalk required for proper villus development in late fetal life (Ramalho-Santos et al., 2000). In addition, Luminal factors are important. Studies of gnotobiotic mice indicate that during postnatal life, members of the commensal microflora play an instructive role in regulating villus

morphology and epithelial gene expression (Hooper et al., 2001).

Members of the Rac GTPase family are potential candidates for processing signals that emanate from the mesenchyme or lumen, and integrating them into pathways that affect intestinal epithelial proliferation and differentiation. Rac1-3 are a subfamily of the Rho GTPases (Mackay and Hall, 1998). Racs play important roles in cellular functions that require focal alterations in actin cytoskeletal organization, such as cell migration and chemotaxis (Nobes and Hall, 1999; Roberts et al., 1999; Chung et al., 2000), assembly of cell junctions (Eaton et al., 1995; Jou et al., 1998, Sussman et al., 2000), exocytosis (Price et al., 1995) and phagocytosis (Caron and Hall, 1998). Depending upon the system studied, Rac signaling can also affect proliferation, differentiation and/or death (Olson et al., 1995; Lores et al., 1997; Li et al., 2000; Mira et al, 2000).

We recently examined the effects of Rac1 activation on mouse intestinal epithelial homeostasis (Stappenbeck and Gordon, 2000). To do so, we generated chimeric mice by introducing genetically manipulated embryonic stem (ES) cells into normal blastocysts. The chimeras contained two populations of intermingled/juxtaposed intestinal epithelial cells. One population was derived from normal blastocysts and provided a reference internal control. The other (experimental) population was derived from ES cells programmed to produce a constitutively active mutant (Rac1Leu61) in descendant intestinal epithelial cells. Expression occurred in both proliferating and differentiating components of the epithelium, beginning at the onset of villus morphogenesis in late fetal life. By comparing the control and experimental cell populations, we determined that Rac1Leu6l signaled precocious differentiation of Paneth cells and enterocytes in the intervillus epithelium. Alterations in apical actin were evident in enterocytes overlying nascent villi (Stappenbeck and Gordon, 2000). Unfortunately, most chimeras expressing the constitutive active mutant died at birth, before completion of crypt-villus morphogenesis. Moreover, we did not know which signaling pathway(s) downstream of Rac produced these effects.

Many potential downstream modulators of Rac GTPases have been described in a number of different, largely ex vivo, experimental systems (Bishop and Hall, 2000). Members of the MAP kinase family have been found to mediate Rac effects on differentiation and migration in two in vivo systems. In the mouse, p38 appears to play a critical role in Rac2-mediated T helper 1 cell differentiation (Li et al., 2000). In *Drosophila*, a Jun N-terminal kinase (Jnk) homolog (BASKET) plays a role downstream of Rac to effect dorsal closure of the embryo. Closure occurs at stages 11-15, as ventral ectodermal cells change shape and migrate to cover the dorsal side of the embryo. Expression of a dominant negative DRAC inhibits movement of leading edge cells (Harden et al., 1995). Inactivating mutations of *basket* and *hemipterous* (homolog of MKK7) phenocopy the defective dorsal closure observed with DRAC inhibition (Riesgo-Escovar et al., 1996; Sluss et al., 1996). These and other observations have led to the proposal that closure involves DRAC signaling through JNK to the nucleus to activate DJUN and subsequently a TGFβ-like pathway (Goberdhan and Wilson, 1998). This Rac-activated pathway appears to promote proper remodeling of the actin cytoskeleton in migrating, leading edge ectodermal cells and to inhibit remodeling in lagging cells.

In this report, we have examined the impact and effectors of Rac1 signaling in the developing and adult mouse small intestinal epithelium of chimeric mice. Rac1 activation proceeds through a pathway that shares some similarities with the one that operates during dorsal closure. p-Jnk induced by Rac1 activation in the small intestinal epithelium is directed to an unusual location: the apical cytoplasm rather than the nucleus. Rac1 activation augments proliferation in the crypt epithelium, and produces remarkable alterations in villus morphology.

MATERIALS AND METHODS

Generation of chimeric mice

A previous report (Stappenbeck and Gordon, 2000) describes construction of p*Fabpl*-Rac1Leu61-*hGH*-*pgk*neo. This plasmid contains nucleotides −596 to +21 of the rat *Fabpl* gene linked to an ORF encoding a human Rac1 mutant (Gln61→Leu; Lamarche et al., 1996) with an N-terminal c-Myc tag, followed by nucleotides +3 to +2150 of the human growth hormone gene (*hGH*) and a *pgk*-neo selection cassette. D3 129/Sv ES cells (Hermiston and Gordon, 1995a) were transfected with purified *Fabpl*-Rac1Leu61-pgk neo DNA. After G418 selection, stably transfected cells were identified by PCR using primers that recognize Rac1 sequences and sequences in exon 2 of *hGH* (5′-AAATACCTGGAGTGCTCGGC-3′; 5′-GACAG-TGTTTGACGAAGCGA-3′, respectively). Cloned Rac1Leu61 ES cell 'lines', or control non-transfected ES cells were then injected into C57Bl/6-ROSA26 (B6-ROSA26) blastocysts (Wong et al., 1998) to produce B6-ROSA26↔129/Sv-Rac1Leu61 chimeric-transgenic mice. Chimeras described in this report were produced from three different *Fabpl*-Rac1Leu61 ES cell lines. Normal chimeras were generated using non-transfected ES cells.

All mice were housed in microisolator cages, in a barrier facility, under a strict 12-hour light cycle. Mice were fed a standard irradiated chow diet (PicoLab Rodent Chow 20, Purina Mills) ad libitum. Mice were maintained in a specified pathogen-free state (i.e. free of Hepatitis, Minute, Lymphocytic Choriomeningitis, Ectromelia, Polyoma, Sendai, Pneumonia, and of mouse adenoviruses, enteric bacterial pathogens and parasites).

Histochemistry

Whole-mount preparations of the small intestine were prepared from adult normal and B6-ROSA26↔129/Sv-Rac1Leu61 chimeras as described (Wong et al., 1998). Periodate-lysine-paraformaldehyde-fixed and X-Gal-stained intestine was embedded in paraffin and 5 μm thick serial sections were prepared, according to protocols reported earlier (Stappenbeck and Gordon, 2000). Sections were stained with nuclear Fast Red, Hematoxylin and Eosin, periodic acid Schiff, Alcian Blue or Phloxine and Tartrazine (Luna, 1968). Adjacent, unstained sections were used for immunohistochemical studies.

Immunohistochemistry

Periodate-lysine-paraformaldehyde-fixed, paraffin-embedded sections of intestine were de-paraffinized with xylene, rehydrated and pre-treated for 15 minutes at room temperature with blocking buffer (1% bovine serum albumin, 0.3% Triton X-100, and 1mM $CaCl_2$ in PBS). Sections of E18.5 or adult small intestine were stained with the following antisera: (1) rabbit anti-human/mouse Rac1 (final dilution in blocking buffer was 1:100; obtained from Santa Cruz Biotechnology, Santa Cruz, CA); (2) mouse anti-c-Myc epitope (1:100; clone 9E10.2; Calbiochem); (3) fluorescein isothiocyanate (FITC)-labeled mouse monoclonal antibodies to β-actin (1:400; clone AC-40; Sigma, St Louis, MO); (4) mouse anti-human Thr183- and Tyr185-phosphorylated Jnk1-3 (recognizes the 46 and 55 kDa forms of p-Jnks 1,2 and 3; 1:100; clone G-7; Santa Cruz Biotechnology); (5) rabbit

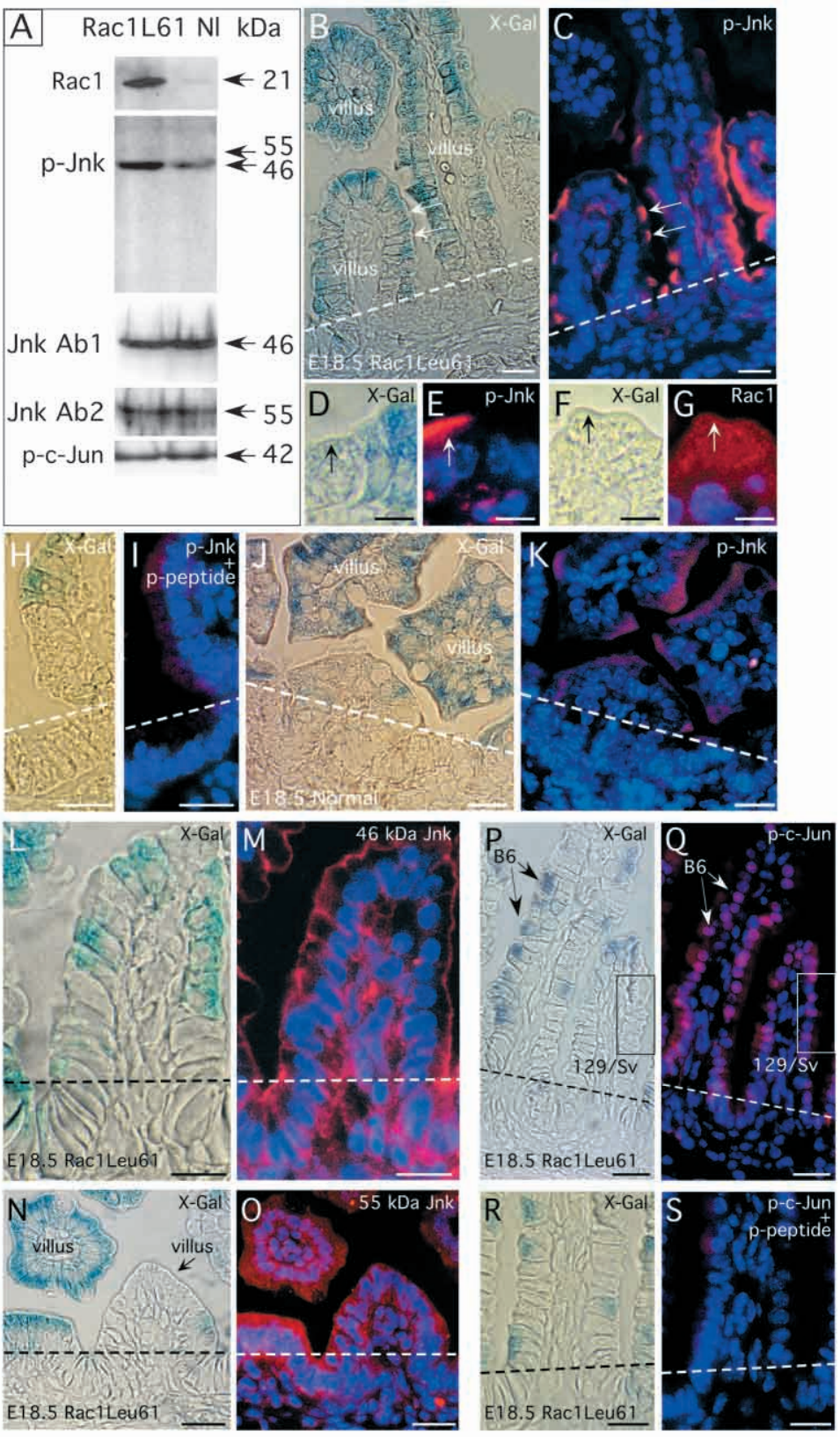

Fig. 1. Increased phosphorylation of 46 kDa Jnk in the apical cytoplasmic compartment of E18.5 129/Sv-Rac1Leu61 intestinal epithelium. (A) Replicate immunoblots of small intestinal extracts (50 μg protein/lane) from E18.5 Rac1Leu61 and normal chimeric mice were probed with antibodies that recognize Rac1, p-Jnk, the 46 kDa or 55 kDa forms of Jnk (designated Jnk-Ab1 and Jnk-Ab2, respectively), and p-c-Jun. (B-S) Sections of E18.5 jejunum from Rac1Leu61 (B-I; L-S) and normal (J,K) chimeric mice. Each antibody staining (C,E,G,I,K,M,O,Q,S) is paired with X-Gal staining (B,D,F,H,J,L,N,P,R) of the same section to show the epithelial cell genotype. At E18.5, the proliferative zone lies in the intervillus region (below broken line) positioned between rudimentary villi (above broken line). Sections from Rac1Leu61 (C,E) and normal chimeric jejunums (K) were stained with rabbit anti-p-Jnk, Cy3-tagged sheep anti-mouse Ig (red) and bis-benzimide (dark blue). 129/Sv epithelial cells in the Rac1Leu61 chimera show markedly enhanced p-Jnk staining localized principally to the apical cytoplasm (arrows). (G) High-power view of 129/Sv villus epithelial cells from a Rac1Leu61 chimera, stained with rabbit anti-Rac1, donkey anti-rabbit Ig and bis-benzamide. Although most of the immunoreactive protein is cytoplasmic, a small fraction localizes to the apical cell surface (arrow). (I) Section from a Rac1Leu61 chimera stained with the same reagents as in C,E, except that the p- Jnk mAb was pre-incubated with phosphorylated Jnk peptide. (M) Section stained with Jnk-Ab1 that recognizes total cellular 46 kDa Jnk, Cy3-tagged donkey anti-rabbit Ig, and bis-benzimide. Jnk (red) localizes to the apical cytoplasm, cell-cell and cell-substrate borders of both 129/Sv-Rac1Leu61 and B6-ROSA26 villus and intervillus epithelial cells. (O) Section incubated with Jnk-Ab2 that recognizes total cellular 55 kDa Jnk, Cy3-labeled donkey anti-rabbit Ig and bis-benzimide. 55 kDa Jnk localizes to the cytoplasm and nuclei of both 129/Sv-Rac1Leu61 and B6-ROSA26 villus and intervillus epithelial cells. (Q) Section stained with mouse anti-p-c-Jun, Cy3-sheep anti-mouse Ig and bis-benzimide. The nuclear staining for p-c-Jun is not appreciably different between the 129/Sv-Rac1Leu61 and B6-ROSA26 epithelial populations (compare B6-ROSA26 cells indicated by arrows to 129/Sv-Rac1Leu61cells indicated by a box). (S) Section from a Rac1Leu61 chimera stained with the same reagents as in Q, except that the p-c-Jun mAb was pre-incubated with phosphorylated c-Jun peptide. Scale bars: B,C,H-S, 25 μm; D-G, 10 μm.

anti-human Jnk1 (raised against Jnk1 but crossreacts with Jnk2 and Jnk3; 1:100; Biosource International, Camarillo, CA); (6) rabbit anti-human Jnk2 (cross reacts with Jnk1 and 3; 1:50; Santa Cruz Biotechnology); (7) mouse anti-human Ser63-phosphorylated c-Jun (1:100; clone KM-1; Santa Cruz Biotechnology); (8) rabbit anti-human c-Jun (1:500; Santa Cruz Biotechnology); (9) mouse anti-human Tyr204-phosphorylated Erk1 and Erk2 (1:100; clone E-4; Santa Cruz Biotechnology); (10) mouse anti-human Tyr182-phosphorylated p38 (1:100; clone D-8; Santa Cruz Biotechnology); (11) rabbit anti-rat p21-activated kinase 1 (Pak1, 1:100; Santa Cruz Biotechnology); (12) rabbit anti-human Tyr215-phosphorylated c-Src (1:100; Biosource International); (13) rabbit anti-human Tyr418-phosphorylated c-Src (1:100, Biosource International; (14) rabbit anti-human Tyr529-phosphorylated c-Src (1:100, Biosource International); (15) mouse anti-human Tyr705 phosphorylated Stat3 (1:50; clone B-7; Santa Cruz Biotechnology); (16) mouse anti-human Stat3 (1:50; clone F-2; Santa Cruz Biotechnology; (17) mouse anti-human NF-κB (1:50; clone F-6; Santa Cruz Biotechnology; (18) mouse anti-CDC47 (1:100; clone 47DC141; NeoMarker, Fremont, CA); and (19) rabbit anti-human cyclin D1 (1:50; Santa Cruz Biotechnology).

Prior to staining with antibodies to Rac1, c-Myc, p-Jnk, p-Erk, p-p38, and p-c-Jun**,** sections were incubated at 95ºC for 15 minutes in 10 mM sodium citrate, pH 6.0. Before incubation with antibodies to β-actin, antigen was retrieved by treating sections with 0.1% chymotrypsin (in 0.1% $CaCl_2$) for 10 minutes at 37°C. Blocking controls were performed for p-Jnk and p-c-Jun staining by pre-incubating each antibody preparation for 1 hour at 24°C with a fivefold molar excess of the corresponding phosphorylated peptide (obtained from Santa Cruz Biotechnology). Antigen-antibody complexes were detected with indocarbocyanine (Cy3)- or FITC-conjugated donkey or sheep anti-rabbit or anti-mouse Ig (1:500, Jackson ImmunoResearch Laboratories, West Grove, PA). Nuclei were stained with bis-benzimide (50 ng/ml PBS).

Immunoblotting

Proteins were extracted (Stappenbeck and Gordon, 2000) from the small intestines of E18.5 Rac1Leu61 and normal chimeras, fractionated by SDS-PAGE (50 μg protein/sample), and transferred to polyvinylidene difluoride membranes. Membranes were then pretreated for 16 hours at 4ºC with blocking buffer (5% powdered nonfat milk in PBS), and probed for 16 hours, at 4ºC with rabbit anti-Rac1 (source listed above; final dilution in blocking buffer was 1:1000). Duplicate blots were probed with mouse anti-human p-Jnk (1:100), rabbit anti-human Jnk 1 (1:2000), rabbit anti-human Jnk 2 (1:2000), mouse anti-human Tyr204-phosphorylated Erk1,2 (1:100), mouse anti-human Tyr182-phosphorylated p38 (1:100), rabbit anti-rat Pak1 (1:500), rabbit anti-human Tyr215-phosphorylated c-Src (1:1000) or mouse anti-human Ser63-phosphorylated c-Jun (1:500). In each case, antigen-antibody complexes were visualized with alkaline phosphatase-conjugated donkey anti-mouse or anti-rabbit Ig, using protocols and reagents provided in the Tropix chemilumiscence detection kit (Tropix, Bedford, MA). Note that a control experiment was used to confirm the specificities of the commercially available p-Jnk and p-c-Jun mAbs. Western blots were prepared containing cellular extracts from a mouse cell line (RAW 264.7; Santa Cruz Biotechnology) known to activate Jnk and c-Jun in response to LPS (Hambleton et al., 1996). The results confirmed the expected LPS-induced increase in levels of 46 kDa and 55 kDa p-Jnk and 42 kDa p-c-Jun.

RESULTS

Chimeric-transgenic mice were produced by injection of genetically manipulated 129/Sv ES cells into B6-ROSA26 blastocysts (Wong et al., 1998). The ES cells had been stably transfected with a recombinant DNA containing transcriptional regulatory elements from a fatty acid-binding protein gene (*Fabpl*) linked to a constitutively active Rac1 mutant (Rac1Leu61; Lamarche et al., 1996). Previous studies showed that expression of transgenes containing these *Fabpl* regulatory elements is initiated by E15, involves all epithelial cells in the intervillus and nascent villus epithelium, and occurs at highest levels in the middle third of the small intestine (jejunum). Expression is sustained throughout adulthood (Hermiston and Gordon, 1995a; Hermiston and Gordon, 1995b; Wong et al., 1998). Chimeras produced using nontransfected ES cells served as controls to evaluate whether B6-ROSA26 and 129/Sv intestinal epithelial cells normally exhibit any strain-specific differences in their properties.

Cytoplasmic Jnk is a target of activated Rac1 in the E18.5 small intestinal epithelium

We began our analysis of the effectors of Rac1 signaling in the intestine by examining expression of the activated forms of three MAP kinase family members: p-Jnk, p-p38 and p-Erk. Embryonic day (E) 18.5 B6-ROSA26↔129/Sv-Rac1Leu61 chimeric-transgenic mice generated with three different cloned, stably transfected *Fabpl*- Rac1Leu61 ES cell lines, and age-matched mice produced from non-transfected ES cells were studied (*n*=3-10 mice/ES cell line/time point).

Rac1Leu61 expression was robust in the intestines of mice generated from each of the three transfected ES cell clones at this developmental stage (see Fig. 1A). Immunoblots of proteins extracted from the entire small intestine of E18.5 B6-ROSA26↔129/Sv-Rac1Leu61 and normal chimeric mice were probed with antibodies that react with the phosphorylated forms of Jnk1, Jnk2 and Jnk3 (p-Jnk). This antibody preparation recognizes both the 46 kDa and 55 kDa forms of each Jnk that are generated through alternative mRNA splicing (Gupta et al., 1996). The immunoblotting results revealed that Rac1Leu61 chimeric-transgenic and normal chimeric mice both contain 46kDa p-Jnk. The relative intensity of the p46kDa Jnk band was reproducibly greater in Rac1Leu61 when compared with normal chimeras (Fig. 1A). A 55 kDa immunoreactive species was only barely detectable in either group, even after prolonged exposure of the probed immunoblots (data not shown).

Replicate immunoblots of mouse intestinal extracts from normal and Rac1Leu61 chimeras were probed with two other antibody preparations: one raised against residues 122-131 of human JNK1, and the other against *Escherichia coli*-derived human JNK2. Both these commercial antibody preparations crossreact with each of the three known mouse Jnks. The antibodies raised against the peptide only recognized 46 kDa Jnk(s) (Jnk Ab1 in Fig. 1A), while the other antibody preparation reacted principally with 55 kDa Jnk(s) (Jnk Ab2 in Fig. 1A). There were no detectable differences in the steady state levels of either 46 kDa or 55 kDa Jnk between normal and Rac1Leu61 chimeras.

Follow-up immunohistochemical studies were performed with the same Jnk antibody preparations to assess the relative cellular levels and intracellular location of 46 kDa p-Jnk, 46 kDa total Jnk and 55 kDa total Jnk in normal and Rac1Leu61-expressing epithelium. B6-ROSA26 cells can be identified based on their production of *E. coli* β-galactosidase (*lacZ*). In contrast, 129/Sv cells are *lacZ* negative. At this stage of gut development, 129/Sv and B6-ROSA26 cells are intermingled in the intervillus and villus epithelium. Sections of small

intestine prepared from E18.5 Rac1Leu61 chimeras were genotyped with X-Gal and stained with p-Jnk antibodies.

The results revealed that 129/Sv-Rac1Leu61 jejunal epithelial cells in both the intervillus and villus compartments contained markedly higher levels of p-Jnk than did neighboring B6-ROSA26 cells (Fig. 1B,C). Thus, the modest increase in the intensity of 46kDa p-Jnk noted in immunoblots (Fig. 1A) underestimated the extent of change in p-Jnk accumulation because only a fraction of the epithelium in these chimeras was 129/Sv-Rac1Leu61. Higher power views show that p-Jnk was localized primarily to the area that underlies the apical cell membrane of 129/Sv-Rac1Leu61 cells, with small amounts of immunoreactive protein positioned at cell-cell borders. Remarkably, there was no detectable nuclear p-Jnk (Fig. 1D,E). Although most immunoreactive Rac1Leu61 is diffusely distributed within the cytoplasm of 129/Sv epithelial cells, higher power views also revealed that a small fraction of the protein is concentrated at the apex of these cells (Fig. 1F,G). The localization of a small portion of total active cellular Rac to areas where downstream responding molecules are present has been described in cultured cells using GFP-labeled Rac1Leu61 and fluorescence resonance energy transfer techniques (Kraynov et al., 2000).

Three additional experiments were performed to demonstrate the specificity of the observed apical/cytoplasmic p-Jnk staining. First, pre-incubation of the p-Jnk mAb with the phosphorylated peptide to which it was raised, abolished the p-Jnk signal in 129/Sv-Rac1Leu61 epithelial cells (Fig. 1H,I). Second, p-Jnk levels and cellular distribution were similar in B6-ROSA26 and 129/Sv jejunal epithelial cells of normal E18.5 chimeras (Fig. 1J,K), indicating that the Rac1-associated effect on p-Jnk seen in Rac1Leu61 epithelial cells can not be ascribed simply to their 129/Sv genetic background. Third, the antibody preparation that recognizes total cellular 46 kDa Jnk (Jnk Ab1) revealed equivalent staining of the area that underlies the apical cell membrane, sites of cell-cell contact and cell-substrate interfaces, but no nuclear staining in Rac1Leu61 chimeras. Importantly, there were no detectable differences in levels or subcellular distribution of 46 kDa Jnk between B6-ROSA26 and 129/Sv-Rac1Leu61 epithelial cells (Fig. 1L,M). Antibodies specific for the 55kDa form of Jnk (Jnk Ab2) disclosed its presence in the nucleus, as well, as its diffuse distribution in the cytoplasm. This was true in both B6-ROSA26 and 129/Sv-Rac1Leu61 intervillus and villus epithelial cells (Fig. 1N,O), emphasizing the uniqueness of the peripheral cytoplasmic location of 46 kDa Jnk.

Together, these findings allowed us to draw the following conclusions. Rac1 activation does not lead to an increase in the total cellular pool of 46 kDa (Fig. 1A), or to its gross intracellular redistribution. However, activation does produce increased phosphorylation of a subset of cellular 46 kDa Jnk in both intervillus and villus epithelial cells. This subset is restricted to a very discrete location within these cells: the area underlying their apical cell membranes.

Functional evidence for the cytoplasmic localization of p-Jnk

Normally, p-Jnk activates c-Jun within the nucleus by phosphorylation of serine residues. The half-life of p-c-Jun increases dramatically, resulting in increased accumulation within the nucleus (Ip and Davis, 1998). Antibodies specific for phosphorylated c-Jun were used to probe immunoblots of proteins extracted from the small intestines of E18.5 Rac1Leu61 and normal chimeras. There were no detectable differences in the levels of p-c-Jun (Fig. 1A). In addition, the same antibodies to p-c-Jun showed that there was no difference in the intensity of nuclear phosphorylated c-Jun staining between E18.5 B6-ROSA26 and 129/Sv intervillus or villus epithelial cells in either chimeric-transgenic or normal chimeric mice (Fig. 1P,Q; data not shown). Nuclear p-c-Jun staining was eliminated in all epithelial cells of the Rac1Leu61 chimeric small intestine when the p-c-Jun mAb was pre-incubated with the phosphorylated peptide to which it had been raised (Fig. 1R,S). Likewise, antibodies that recognize both the phosphorylated and nonphosphorylated forms of c-Jun showed no difference in the accumulation of this p-Jnk substrate in the nuclei of B6-ROSA26 and 129/Sv-Rac1Leu61 epithelial cells (data not shown). These results support our observation that p-Jnk is functionally sequestered in the apical cytoplasm of Rac1Leu61-expressing cells.

Rac1 shows specificity in its activation of MAP kinase family members

To test for the specificity of Rac1Leu61 Jnk activation, we probed immunoblots of small intestinal proteins and sections of small intestine with antibodies specific for the phosphorylated forms of two other MAP kinase family members, Erk1/Erk2, and p38. The immunoblots established that these antibodies react with proteins of the appropriate mass, and that there were no appreciable differences in steady-state levels of either p-Erk1/2 or p-p38 between E18.5 Rac1Leu61 chimeric-transgenic or normal chimeric mice (Fig. 2A; n=3 animals surveyed/group). p-Erk was present throughout the cytoplasm and in the nucleus of both B6-ROSA26 and 129/Sv-Rac1Leu61 epithelial cells. Levels were equivalent in the two populations (Fig. 2B,C). p-p38 had a similar intracellular distribution as p-Erk and levels did not change with Rac1Leu61 expression (data not shown). Thus, neither of these MAP kinases appears to be phosphorylated in a Rac1-dependent fashion to the same degree as Jnk.

Pak1: a potential intermediate in Rac1 activation of Jnk

The intermediate signaling components that connect Rac with Jnk have yet to be definitively determined. Possible candidates include MAP/ERK kinase kinases (MEKK)1 and 4, POSH (Plenty of SH3s), mixed lineage kinases (MLK) 2 and 3, p21-activated kinases (Pak) 1-3 and c-Src (reviewed by Bishop and Hall, 2000).

Immunoblots disclosed that there were no appreciable differences in Pak1 levels between E18.5 normal chimeric and Rac1Leu61 chimeric-transgenic intestine (Fig. 2A). Pak1 shows increased accumulation in the apical cytoplasm of Rac1Leu61-expressing intervillus and villus epithelial cells relative to neighboring B6-ROSA26 cells, where the protein is distributed throughout the cytoplasm (Fig. 2D,E). The localization of Pak1 to the apical cytoplasm is not an effect ascribable to the 129/Sv background, as it was not observed in the 129/Sv epithelium of normal chimeras (Fig. 2F,G). Redistribution of Pak1 from the cytoplasm to plasma membranes occurs with Rac1 activation in cultured fibroblasts (Lu and Mayer, 1999; del Poso et al., 2000). In *Drosophila*,

DPAK localizes to dynamic actin structures in leading edge cells undergoing dorsal closure (Harden et al, 1996). Moreover, activation of Rac1 in mouse cardiomyocytes causes redistribution of Pak1 to the actin cytoskeleton (Sussman et al., 2000). These results are consistent with the notion Pak1 is a downstream target of activated Rac1 in the E18.5 mouse intestinal epithelium.

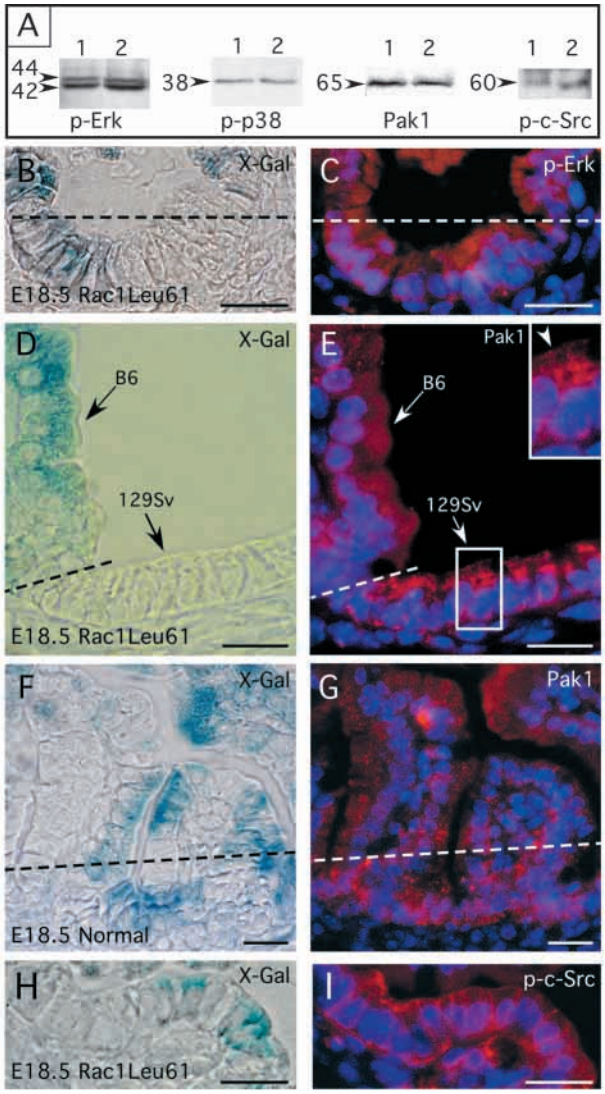

Fig. 2. Rac1Leu61 does not activate other MAP kinases and is associated with Pak1 redistribution in E18.5 mice. (A) Replicate immunoblots of small intestinal extracts from E18.5 Rac1Leu61 and normal chimeric mice (lanes 1 and 2, respectively) were probed with antibodies to p-Erk, p-p38, Pak1, and p215Tyr-c-Src. (B,C) Section from a Rac1Leu61 chimera stained with X-Gal (B) and with mouse anti-p-Erk, Cy3-tagged sheep anti-mouse Ig, plus bis-benzimide (C). There is no detectable difference in nuclear and cytoplasmic staining between neighboring 129/Sv-Rac1Leu61 and B6-ROSA26 epithelial cells. (D-G) Sections from Rac1Leu61 (D,E) and normal (F,G) chimeric jejunum stained with X-Gal and rabbit anti-Pak1, Cy3-donkey anti-rabbit Ig, plus bis-benzimide. E shows that Pak1 staining is more prominent in the apical cytoplasm of 129/Sv-Rac1Leu61 intervillus and villus epithelial cells when, compared with normal adjacent B6-ROSA26 cells (see inset; arrowhead). G shows that Pak1 is diffusely distributed in the cytoplasm of epithelial cells of both genotypes in normal chimeras. (H,I) Intervillus region from a Rac1Leu61 mouse stained with X-Gal and rabbit anti-p215 Tyr-c-Src, Cy3-donkey anti-rabbit Ig, plus bis-benzimide. Rac1Leu61 has no apparent effect on c-Src localization to cell-cell and cell-substrate interfaces. Scale bars: 25 μm.

Activated c-Src has recently been shown to activate DJNK during *Drosophila* embryo closure (Tateno et al., 2000). In addition, c-Src is activated by Rac1 in cardiac muscle (Sussman et al., 2000). Our analysis did not provide any evidence for c-Src-Jnk signal transduction in Rac1Leu61 intestinal epithelium. Immunoreactive p-c-Src was only detectable in the intervillus epithelium, where it was positioned at the cell-cell and cell-substrate interfaces of both 129/Sv and B6-ROSA26 intervillus epithelial cells in E18.5 chimeric-transgenic and normal chimeric mice. The intensity of p-c-Src staining was the same irrespective of cellular genotype (Fig. 2H,I).

Auditing gene function in adult chimeric mice: an internally controlled in vivo experiment

The intervillus epithelium in E18.5 normal chimeras is composed of a mixed population of dividing B6-ROSA26 and 129/Sv cells (e.g. Fig. 2B,F,H). As crypts form during the first two postnatal weeks, a poorly understood 'purification' of the stem cell population occurs so that by postnatal day 14, each crypt in a normal chimeric mouse contains either a wholly B6-ROSA26 or a wholly 129/Sv population of cells (i.e. all active stem cells in mature crypts are of a single genotype, and are presumably descended from a single progenitor that survives the purification process; Wong et al., 1998). As each villus is supplied by several crypts that surround its base, these chimeric mice will contain a subset of villi that are 'polyclonal' (Fig. 3A). A polyclonal villus consists of a coherent vertical column of 129/Sv epithelial cells, extending from a monoclonal 129/Sv crypt up to the villus tip, and an adjacent column of B6-ROSA26 cells emanating from a neighboring monoclonal B6 crypt (Fig. 3A,B). In a chimeric-transgenic mouse, each polyclonal villus represents an internally controlled experiment. The effects of transgene expression can be surmised by comparing the experimental 129/Sv population with the adjacent normal B6-ROSA26 population. Polyclonal villi from adult normal chimeras are used to determine whether any observed differences are simply due to differences between 129/Sv and B6-ROSA26 cells.

Rac1Leu61 perturbs villus architecture in adult chimeras

Chimeric-transgenic mice derived from two of the three Rac1Leu61 ES cell lines typically die shortly after birth without gross histopathological lesions. A total of eight litters were produced with these two cell lines. Only nine B6-ROSA26↔129/Sv-Rac1Leu61 chimeras survived to adulthood (129/Sv contribution to coat color=1-5%). X-Gal staining of whole-mount preparations of jejunum harvested from these nine mice at postnatal day (P) 42 revealed that the 129/Sv contribution to their intestinal epithelium ranged from zero to <0.1%.

In contrast, B6-ROSA26↔129/Sv-Rac1Leu61 chimeras from the third ES cell line survived to at least 9 months of age. These animals had a similar 129/Sv contribution to their coat color as mice produced with the other two lines (i.e. 1-5%). However, they had a higher 129/Sv contribution to their jejunal

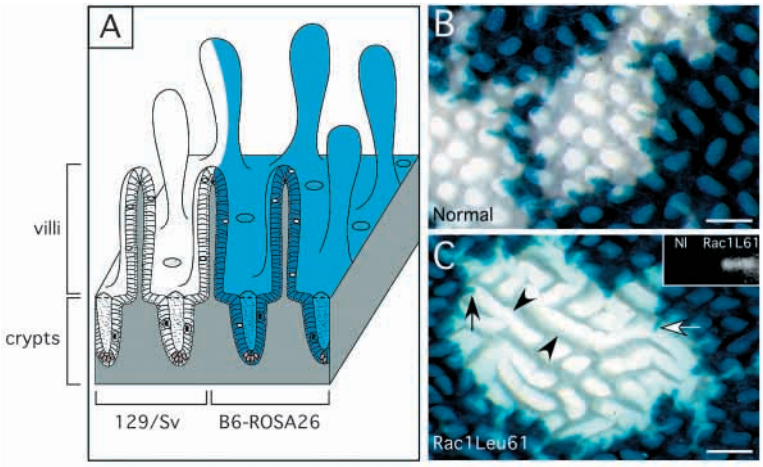

Fig. 3. Rac1Leu61 is associated with markedly widened villi in adult chimeric mice (A) Idealized three-dimensional drawing of the mouse small intestine from a normal C57Bl/6-ROSA26↔129/Sv mouse. The front of the intestine has been 'sectioned' to show the relationship of individual crypts and adjacent villi. In the adult chimeras, crypts are 'monoclonal': composed of either B6-ROSA26 or 129/Sv epithelial cells, but not a mixture of both. Some villi are 'polyclonal': supplied by crypts of both genotype. (B) Whole-mount preparation of jejunum from a 9-month-old normal chimeric mouse. The intestine has been opened, fixed and stained with X-Gal. The white epithelium is 129/Sv. The blue epithelium is composed of B6-ROSA26 cells that express *lacZ*. (C) 9-month-old Rac1Leu61chimeric jejunum prepared as in B. Compared with the normal 129/Sv villi in B, 129/Sv-Rac1Leu61 villi are widened, in some cases coalescing to form very unusual, undulating, slab-like structures (arrowheads). The arrows point to sharply demarcated stripes of blue cells that emanate from B6-ROSA26 crypts supplying two widened polyclonal villi. The inset shows the results of a RT-PCR analysis of normal and Rac1Leu61 RNAs. The 250bp PCR product is from the *Fabpl*-Rac1Leu61 transcript. Scale bars: 235 μm.

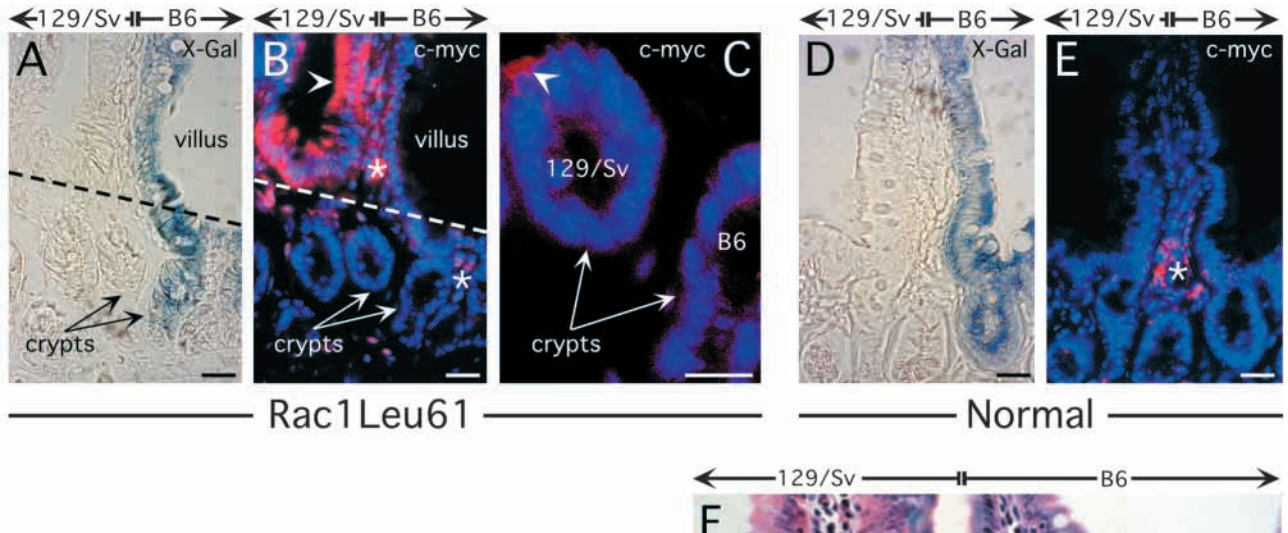

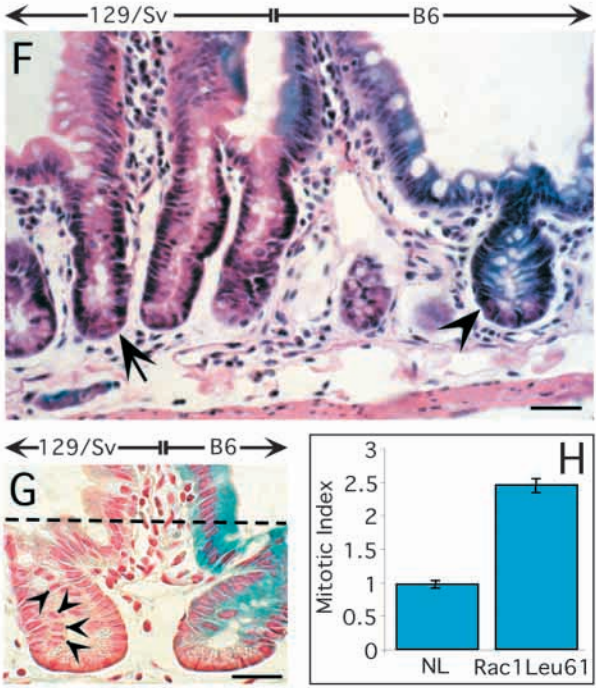

Fig. 4. 129/Sv-Rac1Leu61 crypts in adult chimeric mice are elongated and show increased proliferation. (A-C) Sections from an adult Rac1Leu61 chimeric jejunum. (A) X-Gal genotyping of 129/Sv and B6-ROSA26 epithelial cells. The broken line indicates the location of crypt-villus junctions. (B) Same section as in A stained with mouse anti-c-Myc, Cy3-labeled sheep anti-mouse Ig and bis-benzimide. Cytoplasmic c-Myc staining (red) is more prominent in the 129/Sv villus epithelium (arrowhead) compared with crypt (arrows) epithelium. (C) High-power view of the 129/Sv and adjacent B6 crypts noted in B. The arrowhead highlights the modest increase in c-Myc staining in the upper part of the 129/Sv-Rac1Leu61 crypt compared with the neighboring B6-ROSA26 crypt. (D,E) Section from a normal 9-month-old chimera. (D) X-Gal genotyping. (E) Section stained with the same reagents as in B. Asterisks in B,E indicate Cy3-positive lymphocytes in the lamina propria that react with the mouse secondary antibody. This lamina propria staining can be used as a reference internal control: even with the increased exposure in E, no epithelial c-Myc staining is detectable in the normal chimera. (F,G) X-Gal plus Hematoxylin and Eosin (F), or nuclear Fast Red (G) stained sections. The arrow in F denotes a 129/Sv crypt that appears elongated when compared to a neighboring B6-ROSA26 crypt (arrowhead). In G, arrowheads point to some of the increased M-phase cells present in a 129/Sv crypt. (H) Quantitative morphometric studies reveal a 2.5-fold increase in mitotic index in 129/Sv-Rac1Leu61 crypts. See text for definition of the mitotic index. Scale bars: 25 μm.

epithelium (range=1-5%; *n*=3, examined at 9 months of age). Expression of the *Fabpl*-Rac1Leu61 transgene was verified by RT-PCR of jejunal RNA (Fig. 3C, inset). Each of the 9-month-old Rac1Leu61 chimeras exhibited widening of their 129/Sv but not B6-ROSA26 villi. The widening followed the known cephalocaudal pattern of expression of *Fabpl*- containing transgenes: changes in villus shape were most prominent in the middle third of the small intestine and less significant in the proximal or distal thirds. In each animal, these widened villi appeared to coalesce, forming distinctive undulating slab-like structures in some areas of the jejunum (Fig. 3C). Histological analysis of the widened 129/Sv-Rac1Leu61 villi failed to demonstrate any inflammatory infiltrates or other overt pathological changes in their mesenchymal cores. This phenotype was not a unique feature of this 129/Sv-Rac1Leu61 ES cell line. The rare 129/Sv-Rac1Leu61 jejunal villi encountered in the few surviving P42 mice generated from the other two ES cell lines were also widened relative to neighboring B6-ROSA26 villi. In contrast, widened villi were not observed in any 9-month-old normal chimeras examined (*n*=5; see Fig. 3B).

Surveys of polyclonal villi with widened 129/Sv components (e.g. arrows in Fig. 3C), indicated that the orderly migration of epithelial cells was not grossly disordered. Coherent monophenotypic columns of either B6-ROSA26 or 129/Sv-Rac1Leu61 cells extended from crypts to the tip of these villi. The borders between cellular columns were sharply demarcated.

Immunohistochemical studies using antibodies directed against the c-Myc tag present at the N terminus of Rac1Leu61 revealed that the mutant protein was present in 129/Sv-derived jejunal epithelium and that levels were higher in villi compared to crypts (Fig. 4A,B; *n*=3 9-month-old chimeras). c-Myc staining in epithelial cells located in the upper half of 129/Sv crypts was modestly increased when compared with cells in neighboring B6-ROSA26 crypts (Fig. 4C). Control experiments showed no epithelial staining with the c-Myc antibody in 129/Sv or B6-ROSA26 crypt-villus units of age-matched normal chimeras (Fig. 4D,E).

The majority of the 129/Sv-Rac1Leu61 crypts in 9-month-old chimeras were elongated (up to twofold) when compared with adjacent B6-ROSA26 jejunal crypts (Fig. 4F). This difference was not observed in normal chimeras and thus is not simply a feature of the 129/Sv genetic background. Rac1Leu61-positive crypts contained a greater number of dividing (M-phase) cells (Fig. 4G). The total M-phase cell count for each crypt genotype was determined using an equal number of neighboring 129/Sv and B6-ROSA26 jejunal crypts (*n*=500 well-oriented crypts/genotype/mouse; well-oriented is defined as a sectioned crypt with a unbroken column of epithelial cells extending from its base to the apex of adjacent villi). The quantitative morphometric study produced a mitotic index (ratio of M-phase cells in 129/Sv versus B6-ROSA26 jejunal crypts) that was 2.5-fold increased in Rac1Leu61 mice compared with age-matched normal chimeras (Fig. 4H). The proliferative abnormality did not extend to the villus: M-phase cells were not observed in 129/Sv-Rac1Leu61 epithelium. CDC-47, a marker for S-phase cells, stains >90% of epithelial nuclei located in the middle portion of both 129/Sv and B6-ROSA26 crypts, in normal and Rac1Leu61 chimeras. The modest approx. twofold increase in the number of CDC-47-positive cells in 129/Sv-Rac1Leu61 crypts was directly correlated with the extent of crypt elongation, as was the increase in the number of cyclin D1-positive cells. Cellular levels of cyclin D1 were not appreciably different in 129/SvRac1Leu61 compared with neighboring B6-ROSA26 crypt epithelium (data not shown).

Quantitative morphometric analysis of the same Hematoxylin and Eosin-stained sections used to calculate the mitotic index revealed no significant differences in apoptotic indices between the two groups of animals (data not shown). Thus, it appears that Rac1Leu61 produces an increase in proliferation within crypts without a ‘compensatory’ increase in basal apoptosis. As discussed below, the net increase in crypt cell production could contribute to the abnormal shape of 129/Sv-Rac1Leu61 villi.

These changes in proliferation and villus shape were not associated with notable alterations in cell fate specification. Sections of 129/Sv, B6-ROSA26, and polyclonal jejunal crypt-villus units from adult normal and chimeric-transgenic mice were stained with histochemical reagents, and with well characterized antibodies and lectins that react with differentiating and differentiated members of the goblet, Paneth, enteroendocrine and enterocytic lineages (Falk et al., 1994; Hermiston and Gordon, 1995a; Wong et al., 1998). The results indicated that the fractional representation of each lineage in the crypt and villus epithelium was not obviously perturbed by Rac1Leu61. The proliferative abnormality was not accompanied by dysplasia (see Fig. 4F,G).

Rac1Leu61 affects the cellular distribution of actin and Jnk in adult Rac1Leu61 chimeras

The intracellular location of p-Jnk and Pak1 in E18.5 129/Sv-Rac1Leu61 epithelial cells places them in a strategic position to influence the structure of the actin cytoskeleton. In normal E18.5 chimeras, the bulk of the actin cytoskeleton is localized at the apex of 129/Sv and B6-ROSA26 jejunal villus enterocytes. Rac1Leu61 expression is associated with a modest decrease in apical actin staining that is limited to 129/Sv epithelial cells and not ‘exported’ to juxtaposed normal B6-ROSA26 cells (see Fig. 7 in Stappenbeck and Gordon, 2000).

We used polyclonal villi in adult chimeras to determine whether Rac1 activation had effects on cytoskeletal organization and Jnk phosphorylation/localization that were similar to those observed in the E18.5 intestine. The cytoskeletal effect was similar: β-actin antibodies disclosed a diminution of apical actin staining in the 129/Sv-Rac1Leu component of adult jejunal polyclonal villi (Fig. 5A). This difference between 129/Sv and B6-ROSA26 epithelial cells was not apparent in the jejunal polyclonal villi of 9-month-old normal chimeras (Fig. 5B). As in the E18.5 intestine, antibodies to p-Jnk revealed an increase in the apical cytoplasmic staining in 129/Sv-Rac1Leu61 compared to B6-ROSA26 epithelium (Fig. 5C). Studies of normal chimeras demonstrated that this increase was not an effect of the 129/Sv genetic background (Fig. 5D).

Unlike E18.5 normal chimeras, p-Jnk and Pak1 are detectable in the apical cytoplasm of normal adult 129/Sv and B6-ROSA26 villus epithelial cells (albeit at low levels; see Fig. 5C-E). These differences may reflect the fact that in contrast to late fetal life, endogenous Rac1 is readily detectable in the normal adult mouse villus epithelium (Fig. 5F). Forced

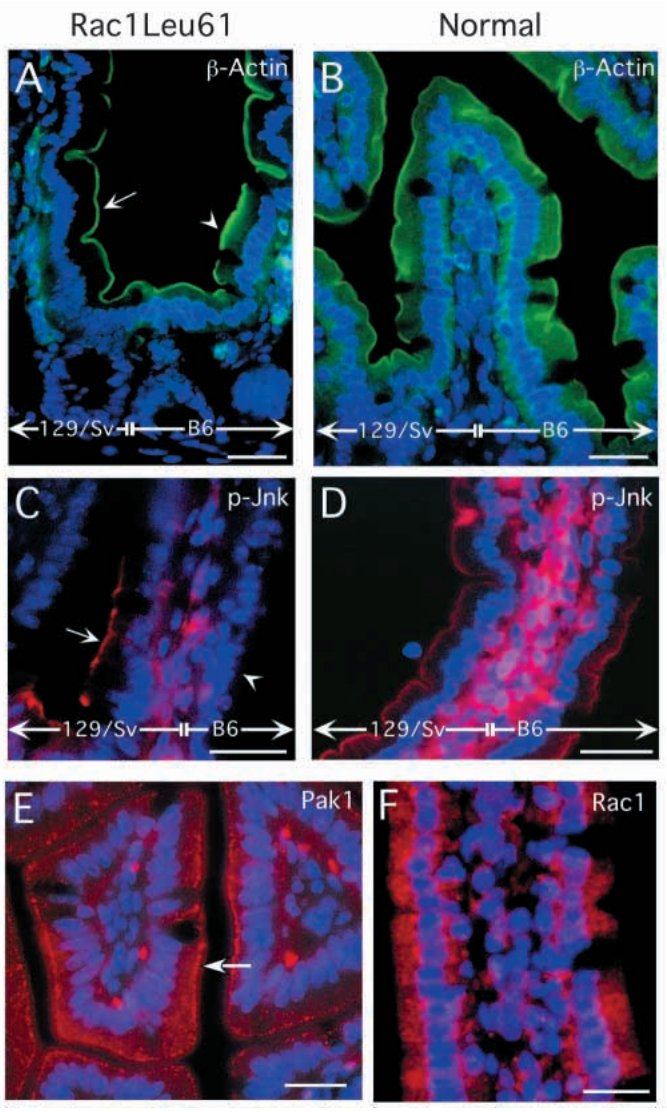

Fig. 5. The effect of Rac1Leu61 on the intracellular epithelial distribution of β-actin and p-Jnk in adult mice. (A) Section containing neighboring 129/Sv and B6-ROSA26 jejunal villi from a 9-month-old Rac1Leu61 chimeric mouse, stained with FITC-labeled mouse anti-β-actin and bis-benzimide. The apical cytoplasmic staining in the 129/Sv-Rac1Leu61villus epithelium (arrow) is diminished relative to the adjacent B6-ROSA26 epithelium (arrowhead). (B) Polyclonal villus from a normal chimera stained with the same reagents as in A. Actin staining is equivalent in 129/Sv and B6-ROSA26 epithelium. (C) Polyclonal villus from an adult chimeric-transgenic mouse stained with mouse anti-p-Jnk, Cy3-labeled sheep anti-mouse Ig and bis-benzimide. The p-Jnk staining is increased in the apical cytoplasm of 129/Sv-Rac1Leu61 villus epithelial cells (arrow) compared to B6-ROSA26 cells (arrowhead). (D) Section from a normal chimeric jejunal villus stained with the same reagents as in C. Increased exposure of D (compare the intensity of staining of lamina propria lymphocytes in C) shows faint but equivalent p-Jnk staining in the cytoplasm of 129/Sv and B6-ROSA26 epithelial cells. (E,F) Pak1 (E) and Rac1 (F) distribution in adult villus epithelium. In E, villi have been sectioned perpendicular to the crypt-villus axis. Pak1 (red) is prominent in the apical cytoplasm of epithelial cells (arrow), irrespective of genotype (B6-ROSA26 cells are shown in this example). Rac1 (red in panel F) is evident throughout the cytoplasm. Scale bars: 25 μm.

expression of Rac1Leu61 does not appear to further augment the apical cytoplasmic pool of Pak1 in adult chimeras (data not shown).

We examined the expression and intracellular distribution of three known downstream components of Rac1 signaling. Nuclear accumulation of p-c-Jun was the same in the 129/Sv-Rac1Leu61 and B6-ROSA26 components of adult polyclonal villi, as it was in E18.5 chimeric-transgenic mice (see above). Rac1 has recently been shown to interact with and activate Stat3 (Signal transducers and activator of transcription 3) in transfected COS-1 cells (Simon et al., 2000). Antibodies that recognize Stat3, or its phosphorylated form, revealed no detectable change in cytoplasmic or nuclear staining with Rac1Leu61 expression in either E18.5 or in adult polyclonal villi (data not shown). Rac1 activation of the NF-κB pathway, potentially through the scaffold protein POSH, leads to nuclear localization of this regulator of pro-inflammatory responses (Tapon et al., 1998). As with Stat3, immunohistochemical studies of E18.5 and 9-month-old chimeric-transgenic and normal chimeric intestine indicated that Rac1Leu61 expression had no detectable effects on NF-κB levels or cellular localization. In addition, antibodies to p-p-38 and p-Erk produced no differences in staining between the 129/Sv and B6-ROSA26 epithelium of E18.5 and adult Rac1Leu61 and normal chimeras (data not shown).

DISCUSSION

We have used chimeric mice to conduct an in vivo analysis of the effects of Rac1 activation on the continuously renewing, simple columnar epithelium of the intestine during and after completion of mouse gut morphogenesis. Our results indicate that expression of a constitutively active human Rac1 mutant leads to accumulation of 46kDa forms of phosphorylated Jnk in the apical cytoplasm, but not in the nucleus, of epithelial cells. The effect is cell autonomous and selective for this member of the MAPK family. The appearance of p-Jnk in the apical cytoplasm is accompanied by the apical cytoplasmic accumulation of Pak1, one of the postulated intermediates in Rac1-mediated activation of Jnk, and by redistribution of actin in the cell periphery. The functional consequences of Rac1 activation in the adult intestinal epithelium include augmented cell proliferation in crypts of Lieberkühn without a change in apoptosis, plus a very unusual distortion of villus architecture.

Our results suggest that an in vivo effect of Rac1 activation in this model epithelium is to modulate p-Jnk-mediated signaling at a distinctive extra-nuclear site. The role of Jnk in stress responses has been characterized extensively in a variety of cultured cell systems (Ip and Davis, 1998). Typically, these stress responses are associated with phosphorylation-dependent localization Jnk to the nucleus, where it activates transcription factors such as c-Jun through Ser/Thr phosphorylation. Two recent papers show that Jnk can be activated in specific cytoplasmic compartments. Almeida et al. (Almeida et al., 2000) observed that culturing rabbit synovial cells on fibronectin leads to activation of a kinase cascade within the focal adhesion. This cascade involves FAK, p130Cas, Ras, Rac1, Pak1 and MEK4, and produces phosphorylated 55 kDa Jnk at the focal adhesion and in the nucleus. McDonald et al. (McDonald et al., 2000) used COS-

7 cells to show that the 55 kDa form of Jnk3 is phosphorylated in cytoplasmic vesicles in response to ligand activation of a G-protein-coupled receptor. Jnk3 activation occurs within a complex that includes β-arrestin 2 plus the upstream activating MAPKKK and MAPKK (ASK1 and MEK4, respectively). Release from this complex appears to allow p-Jnk3 to move to the nucleus. A family of Jnk-interacting proteins (JIP1-3) has been identified that serve as scaffolds for coordinating activation of Jnks in specific cellular compartments (reviewed in Davis, 2000). Other proteins structurally unrelated to the JIP family, such as β-arrestin, may provide an analogous scaffolding function.

The restriction of 46 kDa p-Jnk to the apical cytoplasm of 129/Sv Rac1Leu61 intestinal epithelial cells is intriguing from several perspectives. First, the phosphorylated 46 kDa apical cytoplasmic Jnk represents a component of a more broadly distributed pool of total cytoplasmic 46 kDa Jnk. Our immunohistochemical and immunoblot analyses disclosed that Rac1Leu61 did not produce a detectable change in pool size, or in the intracellular distribution of the pool, but rather a selective phosphorylation of its apical cytoplasmic component. One implication of these observations is that this epithelium may contain as yet unspecified JIP-like molecules that can function to direct Rac1-activated Jnk phosphorylation in the apical cytoplasm. Second, the cytoplasmic p-Jnk is not the 55 kDa form described in synovial or COS-7 cells (see above). 46 kDa Jnks contain a truncated C terminus, owing to alternative splicing (Gupta et al., 1996). Our findings raise the possibility that information encoded in the C-terminal tail of Jnk may help define its cytoplasmic versus nuclear localization/function. Third, this is the first report of the in vivo effects of Rac1 activation on p-Jnk localization in a mammalian system. It will therefore be important to determine whether cytoplasmic restriction of (46 kDa) p-Jnk is a general feature of epithelial responses to Rac1 activation, and whether other, non-epithelial, lineages support comparable responses in vivo.

Our studies reveal that Rac1Leu61 causes reorganization of actin in the periphery of intestinal epithelial cells in a cell autonomous fashion. Based on this finding, we hypothesize that p-Jnk localized to the periphery can act directly on cytoplasmic proteins to effect this reorganization. In *Drosophila*, SPIRE, which has WH2 domains homologous to mammalian Wiscott-Aldrich syndrome proteins (WASP), binds to both Rac GTPase and actin. Mutants of *spire* phenocopy the effects of cytochalasin D treatment, leading to the proposal that *spire* encodes a protein involved in regulating the actin cytoskeleton (Wellington et al., 1999). In addition, this protein is phosphorylated by DJNK, providing a possible link between Rac activity and effects on actin organization (Otto et al., 2000). A mouse EST with homology to SPIRE has been identified (GenBank Accession Number, W54692; see Wellington et al., 1999). Using this sequence and RT-PCR assay spanning an intron-exon junction of the gene, we have found that this putative ortholog is produced throughout the length of the small intestine and colon. It will be interesting to define its cellular and intracellular locations, in normal and Rac1Leu61 chimeric intestine once an antibody suitable for immunochemistry is available.

Rac1 does not directly activate Jnk. Studies in yeast and cultured mammalian cells indicate that a number of molecules including MEK kinase 1 and 4, p21-activated kinases, POSH and MLK2,3 are capable of mediating Rac activation of Jnk (Bishop and Hall, 2000). PAK and MEKK appear to activate Jnk through independent pathways (Fanger et al., 1997; Xia et al., 2000). Rac1-activation of p-Jnk in the mouse intestinal epithelium is associated with accumulation of apical cytoplasmic Pak1. This may be coincidence, or it may reflect operation of Rac-Pak-MEK4-Jnk signaling in this epithelium in vivo. To date, we have been unable to detect a specific signal for MEK kinase in either E18.5 or adult normal or chimeric-transgenic mouse intestine using commercially available antibodies, sensitive fluorescence detection systems, and a variety of antigen retrieval procedures (data not shown).

Previous loss-of-function genetic experiments had not identified a function for Jnks in the gut epithelium. Mice deficient in either Jnk1 or Jnk2 do not have any reported histopathological changes in their intestine. The principal phenotype is a defect in T-cell differentiation (Dong et al., 1998; Yang et al., 1998). Compound homozygous $Jnk1^{-/-}$, $Jnk2^{-/-}$ mice die by E12.5 with severe hindbrain exencephaly, well before initiation of villus and crypt morphogenesis (Kuan et al., 1999). Jnk3 expression is restricted to brain, heart and testes: knockout animals have abnormal apoptotic responses in the hippocampus (Yang et al., 1997).

Our gain-of-function experiment in adult chimeric mice reveals that Rac1/Jnk activation is associated with increased intestinal epithelial proliferation, and a marked abnormality in villus architecture. This response differs from that observed during late fetal life. Unlike the adult crypt, the intervillus epithelium of E18.5 mice supports high levels of Rac1Leu61 expression, and displays precocious differentiation of Paneth cells and enterocytes (Stappenbeck and Gordon, 2000). These differences may reflect a number of factors, including the marked difference in levels of activated Rac expression.

There are three notable features of the proliferative abnormality observed in adult mice: (1) it is restricted to crypts and does not extend to villi; (2) it is not accompanied by an increase in basal apoptotic rates within the crypt; and (3) there is no accompanying cellular dysplasia. The mechanisms underlying the proliferative response in intestinal crypts are undoubtedly complex. Analyses of a variety of cultured cell systems have disclosed extensive cross-talk between Rac, Ras and Rho GTPases, and regulatory components of the cell cycle (Bar-Sagi and Hall, 2000).

The determinants of villus development and shape are poorly understood. As noted in the Introduction, recent studies by Karlsson et al. (Karlsson et al., 2000) indicate that villus formation is initiated in fetal life through an epithelial-mesenchymal crosstalk involving PDGF-A and PDGF receptor α. The villus architectural abnormality associated with expression of Rac1Leu61 in adult mice is very unusual. We know of no other report where a genetic or hormonal manipulation has produced such pronounced widening of villi, without any histopathological changes in the mesenchymal core of the villus. Increased crypt cell proliferation without a compensating apoptotic response, as observed in 129/Sv-Rac1Leu61 crypts, is known to produce increased epithelial cell census in crypt-villus units. However, in other mouse models, these census increases are usually manifested by elongated crypts, increases in villus length, or by villus

bifurcation, but not by generation of such dramatically widened villi (Druker et al., 1996; Wong et al., 1998).

One interpretation of the widened villus phenotype is that it reflects actin cytoskeletal changes induced by Rac1Leu61 and associated Jnk activation. In this scenario, the epithelium functions as a major determinant of the widened villus architecture, either as a result of changes in its physical properties, or as a result of Rac-dependent changes epithelial-mesenchymal crosstalk. Increased crypt cell proliferation, unaccompanied by augmented apoptosis, may also contribute to the widened phenotype, but is unlikely to be the sole cause, based on the shape of villi in other mouse models with augmented crypt cell production. The idea that Rac1 signaling in the epithelium can influence villus shape warrants further investigation. Understanding the underlying mechanisms may provide insights about the factors that allow mature villi to maintain their normal shape in the face of continuous renewal of their overlying epithelium.

We thank David O'Donnell, Maria Karlsson and Sabrina Wagoner for their expert technical assistance, and Melissa Wong for her many helpful comments. This work was supported by NIH grants DK30292 and DK02954.

REFERENCES

Almeida, E. A. C., Ilic, D., Han, Q., Hauck, C. R., Jin, F., Kawakatsu, H., Schlaepfer, D. D. and Damsky, C. H. (2000). Matrix survival signaling: from fibronectin via focal adhesion kinase to c-Jun NH_2-terminal kinase. *J. Cell Biol.* **149**, 741-754.

Bar-Sagi, D. and Hall, A. (2000). Ras and Rho GTPases: a family reunion. *Cell* **103**, 227-238.

Bishop, A. L. and Hall, A. (2000). Rho GTPases and their effector proteins. *Biochem. J.* **348**, 241-255.

Bjerknes, M. and Cheng, H. (1999). Clonal analysis of mouse intestinal epithelial progenitors. *Gastroenterology* **116**, 7-14.

Booth, C. and Potten, C. S. (2000). Gut instincts: thoughts on intestinal epithelial stem cells. *J. Clin. Invest.* **105**, 1493-1499.

Bry, L., Falk, P., Huttner, K., Ouellette, A., Midvedt, T. and Gordon, J. I. (1994). Paneth cell differentiation in the developing intestine of normal and transgenic mice. *Proc. Natl. Acad. Sci. USA.* **91**, 10335-10339.

Calvert, R. and Pothier, P. (1990). Migration of fetal intestinal intervillous cells in neonatal mice. *Anat. Rec.* **227**, 199-206.

Caron, E. and Hall, A. (1998). Identification of two distinct mechanisms of phagocytosis controlled by different Rho GTPases. *Science* **282**, 1717-1721.

Cheng, H. (1974a). Origin, differentiation, and renewal of the four main epithelial cell types in the mouse small intestine. II. Mucous cells. *Am. J. Anat.* **141**, 481-502.

Cheng, H. (1974b). Origin, differentiation, and renewal of the four main epithelial cell types in the mouse small intestine. IV. Paneth cells. *Am. J. Anat.* **141**, 521-536.

Cheng, H. and Leblond, C. P. (1974a). Origin, differentiation, and renewal of the four main epithelial cell types in the mouse small intestine. I. Columnar cells. *Am. J. Anat.* **141**, 461-480.

Cheng, H. and Leblond, C. P. (1974b). Origin, differentiation, and renewal of the four main epithelial cell types in the mouse small intestine. III. Entero-endocrine cells. *Am. J. Anat.* **141**, 503-520.

Cheng, H. and Leblond, C. P. (1974c). Origin, differentiation, and renewal of the four main epithelial cell types in the mouse small intestine. V. Unitarian theory of the origin of the four epithelial cell types. *Am. J. Anat.* **141**, 537-561.

Chung, C. Y., Lee, S., Briscoe, C., Ellsworth, C. and Firtel, R. A. (2000). Role of Rac in controlling the actin cytoskeleton and chemotaxis in motile cells. *Proc. Natl. Acad. Sci. USA* **97**, 5225–5230.

Davis, R. J. (2000). Signal transduction by the JNK group of MAP kinases. *Cell* **103**, 239-252.

del Pozo, M. A., Price, L. S., Alderson, N. B., Ren, X.-D. and Schwartz, M. A. (2000). Adhesion to the extracellular matrix regulates the coupling of the small GTPase Rac to its effector PAK. *EMBO J.* **9**, 2008-2014.

Dong, C., Yang, D. D., Wysk, M., Whitmarsh, A. J., Davis, R. J. and Flavell, R. A. (1998). Defective T cell differentiation in the absence of Jnk1. *Science* **282**, 2092-2095.

Drucker, D. J., Ehrlich, P., Asa, S. L. and Brubaker, P. L. (1996). Induction of intestinal epithelial proliferation by glucagon-like peptide 2. *Proc. Natl. Acad. Sci. USA* **93**, 7911-7916.

Eaton, S., Auvinen, P., Luo, L., Jan, Y. N. and Simons, K. (1995). CDC42 and Rac1 control different actin-dependent processes in the *Drosophila* wing disc epithelium. *J. Cell Biol.* **131**, 151-164.

Falk, P., Roth, K A. and Gordon, J. I. (1994). Lectins are sensitive tools for defining the differentiation programs of mouse gut epithelial cell lineages. *Am. J. Physiol.* **266**, G987-G1003.

Fanger, G. R., Johnson, N. L. and Johnson, G. L. (1997). MEK kinases are regulated by EGF and selectively interact with Rac/Cdc42. *EMBO J.* **16**, 4961-4972.

Goberdhan, D. C. I. and Wilson, C. (1998). JNK, cytoskeletal regulator and stress response kinase? A *Drosophila* perspective. *BioEssays* **20**, 1009-1019.

Gupta, S., Barrett, T., Whitmarsh, A. J., Cavanagh, J., Sluss, H. K., Derijard, B. and Davis, R. J. (1996). Selective interaction of JNK protein kinase isoforms with transcription factors. *EMBO J.* **15**, 2760-2770.

Hall, P. A., Coates, P. J., Ansari, B. and Hopwood, D. (1994). Regulation of cell number in the mammalian gastrointestinal tract: the importance of apoptosis. *J. Cell Sci.* **107**, 3569-3577.

Hambleton, J., Weinstein, S. L., Lem, L. and DeFranco, A. L. (1996). Activation of c-Jun N-terminal kinase in bacterial lipopolysaccharide-stimulated macrophages. *Proc. Natl. Acad. Sci. USA* **93,** 2774-2778.

Harden, N., Loh, H. Y., Chia, W. and Lim, L. (1995). A dominant inhibitory version of the small GTP-binding protein Rac disrupts cytoskeletal structures and inhibits developmental cell shape changes in *Drosophila*. *Development* **121**, 903-914.

Harden, N., Lee, J., Loh, H. Y., Ong, Y. M., Tan, I., Leung, T., Manser, E. and Lim, L. (1996). A *Drosophila* homolog of the Rac-and Cdc42-activated serine/threonine kinase PAK is a potential focal adhesion and focal complex protein that colocalizes with dynamic actin structures. *Mol. Cell. Biol.* **16**, 1896-1908.

Hermiston, M. L. and Gordon, J. I. (1995a). In vivo analysis of cadherin function in the mouse small intestinal epithelium: essential role in adhesion, maintenance of differentiation, and regulation of programmed cell death. *J. Cell Biol.* **129**, 489-506.

Hermiston, M. L. and Gordon, J. I. (1995b). Inflammatory bowel disease and adenomas in mice expressing a dominant negative N-cadherin. *Science* **270**, 1203-1207.

Hooper, L. V., Wong, M. H., Thelin, A., Hansson, L., Falk, P. G. and Gordon, J. I. (2001) Molecular analysis of commensal host-microbial relationships in the intestine. *Science* **291**, 881-884.

Ip, Y. T. and Davis, R. J. (1998). Signal transduction by the c-Jun N-terminal kinase (JNK)-from inflammation to development. *Curr. Opin. Cell Biol.* **10**, 205-219.

Jou, T. S., Schneeberger, E. E. and Nelson, W. J. (1998). Structural and functional regulation of tight junctions by RhoA and Rac1 small GTPases. *J. Cell Biol.* **142**, 101-115.

Karlsson, L., Lindahl, P., Heath, J. K. and Betsholtz, C. (2000). Abnormal gastrointestinal development in PDGF-A and PDGFR-α deficient mice implicates a novel mesenchymal structure with putative instructive properties in villus morphogenesis. *Development* **127**, 3457-3466.

Kraynov, V. S., Chamberlain, C., Bokoch, G. M., Schwartz, M. A., Slabaugh, S. and Hahn, K. M. (2000). Localized Rac activation dynamics visualized in living cells. *Science* **290**, 333-337.

Kuan, C.-Y., Yang, D. D., Samanta Roy, D. R., Davis, R. J., Rakic, P. and Flavell, R. A. (1999). The Jnk1 and Jnk2 protein kinases are required for regional specific apoptosis during early brain development. *Neuron* **22**, 667-676.

Lamarche, N., Tapon, N., Stowers, L., Burbelo, P. D., Aspenström, P., Bridges, T., Chant, J. and Hall, A. (1996). Rac and Cdc42 induce actin polymerization and G1 cell cycle progression independently of p65PAK and the JNK/SAPK MAP kinase cascade. *Cell* **87**, 519-529.

Li, B., Yu, H., Zheng, W.-P., Voll, R., Na, S., Roberts, A. W., Williams, D. A., Davis, R. J., Ghosh, S. and Flavell, R. A. (2000). Role of the guanosine triphosphatase Rac2 in T helper 1 cell differentiation. *Science* **288**, 2219-2222.

Lores, P., Morin, L., Luna, R. and Gacon, G. (1997). Enhanced apoptosis in the thymus of transgenic mice expressing constitutively activated forms of human Rac2 GTPase. *Oncogene* **15**, 601-605.

Lu, W. and Mayer, B. J. (1999). Mechanism of activation of Pak1 kinase by membrane localization. *Oncogene* **18**, 797-806.

Luna, L. G. (1968). *Manual of Histologic Staining Methods of the Armed Forces Institute of Pathology*. New York: McGraw-Hill.

Mackay D. J. and Hall, A. (1998). Rho GTPases. *J. Biol. Chem.* **273**, 20685-20688.

McDonald, P. H., Chow, C.-W., Miller, W. E., Laporte, S. A., Field, M. E., Lin, F.-T., Davis, R. J. and Lefkowitz. R. J. (2000). β-Arrestin-2: a receptor-regulated MAPK scaffold for the activation of JNK3. *Science* **290**, 1574-1577.

Mira J. P., Benard, V., Groffen, J., Sanders, L. C. and Knaus, U. G. (2000). Endogenous, hyperactive Rac3 controls proliferation of breast cancer cells by a p21-activated kinase-dependent pathway. *Proc. Natl. Acad. Sci. USA* **97**, 185-189.

Nobes, C. D. and Hall, A. (1999). Rho GTPases control polarity, protrusion, and adhesion during cell movement. *J. Cell Biol.* **144**, 1235-1244.

Olson, M. F., Ashworth, A. and Hall, A. (1995). An essential role for Rho, Rac, and Cdc42 GTPases in cell cycle progression through G_1. *Science* **269**, 1270-1272.

Otto, I. M., Raabe, T., Rennefahrt, U. E. E., Bork, P., Rapp, U. R. and Kerkhoff, E. (2000). The p150-Spir protein provides a link between c-Jun N-terminal kinase function and actin reorganization. *Curr. Biol.* **10**, 345-348.

Price L. S., Norman, J. C., Ridley, A. J. and Koffer, A. (1995). The small GTPases Rac and Rho as regulators of secretion in mast cells. *Curr. Biol.* **5**, 68-73.

Ramalho-Santos, M., Melton, D. A. and McMahon, A. P. (2000). Hedgehog signals regulate multiple aspects of gastrointestinal development. *Development* **127**, 2763-2772.

Riesgo-Escovar, J. R., Jenni, M., Fritz, A. and Hafen, E. (1996). The *Drosophila* Jun N-terminal kinase is required for cell morphogenesis but not for DJun-dependent cell fate specification in the eye. *Genes Dev.* **10**, 2759-2768.

Roberts, A. W., Kim, C., Zhen, L., Lowe, J. B., Kapur, R., Petryniak, B., Spaetti, A., Pollock, J. D., Borneo, J. B., Bradford, G. B., Atkinson, S. J., Dinauer, M. C. and Williams, D. A. (1999). Deficiency of the hematopoietic cell-specific Rho family GTPase Rac2 is characterized by abnormalities in neutrophil function and host defense. *Immunity* **10**, 183-196.

Schmidt, G. H., Wilkinson, M. M. and Ponder, B. A. (1985). Cell migration pathway in the intestinal epithelium: an *in situ* marker system using mouse aggregation chimeras. *Cell* **40**, 425-429.

Schmidt, G. H., Winton, D. J. and Ponder, B. A. (1988). Development of the pattern of renewal in the crypt-villus unit of chimaeric mouse small intestine. *Development* **103**, 785-790.

Simon, A. R., Vikis, H. G., Stewart, S., Fanburg, B. L., Cochran, B. H. and Guan, K.-L. (2000). Regulation of STAT3 by direct binding of Rac1 to the GTPase. *Science* **290**, 144-147.

Sluss, H. K., Han, Z., Barrett, T., Davis, R. J. and Ip, Y. T. (1996). A JNK signal transduction pathway that mediates morphogenesis and an immune response in *Drosophila*. *Genes Dev.* **10**, 2745-2758.

Stappenbeck, T. S. and Gordon. J. I. (2000). Rac1 mutations produce aberrant epithelial differentiation in the developing and adult mouse small intestine. *Development* **127**, 2629-2642.

Sussman, M. A., Welch, S., Walker, A., Klevitsky, R., Hewett, T. E., Price, P. L., Schaefer, E. and Yager, K. (2000). Altered focal adhesion regulation correlates with cardiomyopathy in mice expressing constitutively active rac1. *J. Clin. Invest.* **105**, 875-886.

Tapon, N., Nagata, K.-I., Lamarche, N. and Hall, A. (1998). A new Rac target POSH is an SH3-containing scaffold protein involved in the JNK and NF-κB signaling pathways. *EMBO J.* **17**, 1395-1404.

Tateno, M., Nishida, Y. and Adachi-Yamada,T. (2000). Regulation of JNK by Src during *Drosophila* development. *Science.* **287**, 324-327.

Wellington, A., Emmons, S., James, B., Calley, J., Grover, M., Tolias, P. and Manseau, L. (1999). Spire contains actin binding domains and is related to ascidian posterior end mark-5. *Development* **126**, 5267-5274.

Wong, M. H., Rubinfeld, B. and Gordon, J. I. (1998). Effects of forced expression of an NH_2-terminal truncated β-catenin on mouse intestinal epithelial homeostasis. *J. Cell Biol.* **141**, 765-777.

Wong, M. H., Saam, J. R., Stappenbeck, T. S., Rexer, C. H. and Gordon, J. I. (2000). Genetic mosaic analysis based on Cre recombinase and navigated laser capture microdissection. *Proc. Natl. Acad. Sci. USA* **97**, 12601-12606.

Xia, Y., Makris, C., Su, B., Li, E., Yang, J., Nemerow, G. R. and Karin, M. (2000). MEK kinase 1 is critically required for c-Jun N-terminal kinase activation by proinflammatory stimuli and growth factor-induced cell migration. *Proc. Natl. Acad. Sci. USA* **97**, 5243-5248.

Yang, D. D., Kuan, C.-Y., Whitmarsh, A. J., Rincon, M., Zheng, T. S., Davis, R. J., Rakic, P. and Flavell, R. A. (1997). Absence of excitotoxicity-induced apoptosis in the hippocampus of mice lacking the Jnk3 gene. *Nature* **389**, 865-870.

Yang, D. D., Conze, D., Whitmarsh, A. J., Barrett, T., Davis, R. J., Rincon, M. and Flavell, R. A. (1998). Differentiation of CD4+ T cells to Th1 cells requires MAP kinase JNK2. *Immunity* **9**, 575-585.